RSC Advances

PAPER

View Article Online
View Journal | View Issue

Check for updates

Cite this: *RSC Adv.*, 2022, **12**, 3073

A salicylaldehyde benzoyl hydrazone based near-infrared probe for copper(II) and its bioimaging applications†

Jie Zhao,‡[a] Yue-yuan Wang,‡[a] Wen-ling Chen,[b] Guang-shu Hao,[a] Jian-ping Sun,[a] Qing-fang Shi,[a] Fang Tian*[a] and Run-tian Ma *[b]

Received 24th November 2021
Accepted 15th January 2022

DOI: 10.1039/d1ra08616b

rsc.li/rsc-advances

Developing highly sensitive and selective methods for Cu^{2+} detection in living systems is of great significance in clinical copper-related disease diagnosis. In this work, a near infrared (NIR) fluorescent probe, CySBH, with a salicylaldehyde benzoyl hydrazone group as a selective and sensitive receptor for Cu^{2+} was designed and synthesized. The specific coordination of the salicylaldehyde benzoyl hydrazone group in CySBH with Cu^{2+} can induce a distinct quench of the fluorescence intensity, allowing for real-time tracking of Cu^{2+}. We have demonstrated that CySBH could rapidly recognize Cu^{2+} with good selectivity and high sensitivity. Moreover, on the basis of low cell cytotoxicity, the probe was used to visualize Cu^{2+} in two cell lines by fluorescence imaging. Furthermore, CySBH can also be used to monitor Cu^{2+} *in vivo* due to its NIR emission properties. These overall results illustrate that the NIR fluorescent probe CySBH provides a novel approach for the selective and sensitive monitoring of Cu^{2+} in living systems.

1. Introduction

Copper(II) ions (Cu^{2+}) are the third most abundant transition metal ions in the human body and play significant roles in various fundamental physiological processes, such as detoxifying oxygen-derived radicals, signal transduction and coagulating blood.[1–3] Excess accumulation of Cu^{2+} in the body can lead to serious consequences, such as cellular damage, Menkes disease, Wilson disease, cancer, cardiovascular disorders, Alzheimer's disease and even death.[4–6] Therefore, maintaining Cu^{2+} at appropriate concentrations is vital for the growth and fitness of living organisms. Given the significance of copper to human health, the selective and sensitive monitoring of Cu^{2+} ions in living systems is of great importance to evaluate copper-related diseases.

In recent years, many methods, such as inductively coupled plasma-mass spectrometry,[7,8] electrochemical and electrochemical luminescence sensors,[9–11] colorimetric methods[12,13] and fluorescent detection,[14–17] have been successfully developed for the detection of Cu^{2+}. Among them, technology based on fluorescence probes has become one of the most important methods to detect Cu^{2+} in living systems because of its quick response, high sensitivity, low detection limit reliability and low cost.[18–21] Great efforts have been made in the development of novel fluorescence probes for Cu^{2+} detection. Additionally, fluorescence probes in the near-infrared window (NIR, 650–900 nm) have attracted great interest due to their incomparable advantages, such as low auto-fluorescence of biosystems and deep penetration into tissue.[22–26] To date, various NIR fluorescence probes with different recognition mechanisms have been designed and used for Cu^{2+} detection.[27–30] One of the most important approaches to design NIR fluorescent probes for copper ion detection is to graft a Cu^{2+} selective receptor unit to the fluorophore.[31,32] For example, Li *et al.* developed a NIR fluorescence probe bearing 2-(1*H*-benzo[*d*]imidazol-2-yl)-phenol as a copper ion receptor.[33] Zhang *et al.* described a 2-picolinic ester-based NIR probe, NIR-Cu, for monitoring Cu^{2+} *in vivo*.[34] Tang's group developed a NIR fluorescent copper probe and successfully applied it to visualize Cu^{2+} in living cells, rat hippocampal tissues and zebrafish models.[35] In addition, some probes can recognize Cu^{2+} based on rhodamine by a closed-state spiro ring.[36,37] However, due to the limitations of the recognition group in selectivity and sensitivity, those probes still encounter some problems, such as poor selectivity, slow response and poor photostability.[38,39] Therefore, the development of novel NIR fluorescent probes with selective and sensitive receptors for Cu^{2+} would be of great value.

Salicylidene acylhydrazone Schiff bases are one of most important π-conjugated ligands for Cu^{2+}. In addition, these

[a]*Gansu Provincial Maternity and Child-care Hospital, Lanzhou 730000, Gansu Province, P. R. China. E-mail: tianfang720203@163.com*

[b]*College of Science, Gansu Agricultural University, Lanzhou 730000, Gansu Province, P. R. China. E-mail: mart@gsau.edu.cn*

† Electronic supplementary information (ESI) available: Table S1, Fig. S1–S4, NMR and HRMS spectra of synthetic compounds. See DOI: 10.1039/d1ra08616b

‡ These authors contributed equally to this work and are both considered to the first author.

Open Access Article. Published on 24 January 2022. Downloaded on 2/11/2026 10:11:22 PM. This article is licensed under a Creative Commons Attribution-NonCommercial 3.0 Unported Licence.

Open Access Article. Published on 24 January 2022. Downloaded on 2/11/2026 10:11:22 PM.
This article is licensed under a Creative Commons Attribution-NonCommercial 3.0 Unported Licence.

compounds display keto–enol tautomerism, and both the nitrogen atom and oxygen atom in the Schiff bases can act as ligand donors for Cu^{2+} and consequently produce stable coordination complexes *via* coordination effects.[40,41] The phenol group in phenol-based Schiff base units is deprotonated in the coordination process, which could diminish the electron-donating ability of the oxygen atom.[42–46] Moreover, it has been reported that the fluorescence signal of hemicyanine-based NIR fluorophores could be turned in a controllable manner by diminishing the electron-donating ability of the oxygen atom in its phenol group. Therefore, a hemicyanine-based NIR fluorescent probe using salicylidene acylhydrazone Schiff bases as a selective recognition group has great potential in the selective recognition of Cu^{2+}.

In this study, we proposed a novel Cu^{2+} detection probe, CySBH, in which an important NIR fluorophore hemicyanine was connected with benzoyl hydrazine *via* an imine bond. The phenolic hydroxyl and acyl hydrazone groups in CySBH tactfully formed a special salicylaldehyde benzoyl hydrazone group. The salicylaldehyde benzoyl hydrazone group is known to be a good coordinating site for Cu^{2+} due to the imine nitrogen atom, amide oxygen atom and phenolic hydroxyl oxygen atom, which could be used as a selective coordination unit for Cu^{2+} (Scheme 1a). In the presence of Cu^{2+}, the salicylaldehyde benzoyl hydrazone group on CySBH can effectively coordinate with copper ions, resulting in the NIR fluorescent signal of CySBH being quenched. The responses of CySBH toward Cu^{2+} were fully proven by UV-vis absorption, fluorescence and mass analysis. Furthermore, we also demonstrated that CySBH can react with intracellular Cu^{2+} and effectively turn off fluorescence in living cells and mice. Such fluorescence responses of CySBH in this work provide a novel approach for the selective and sensitive monitoring of Cu^{2+} in living systems.

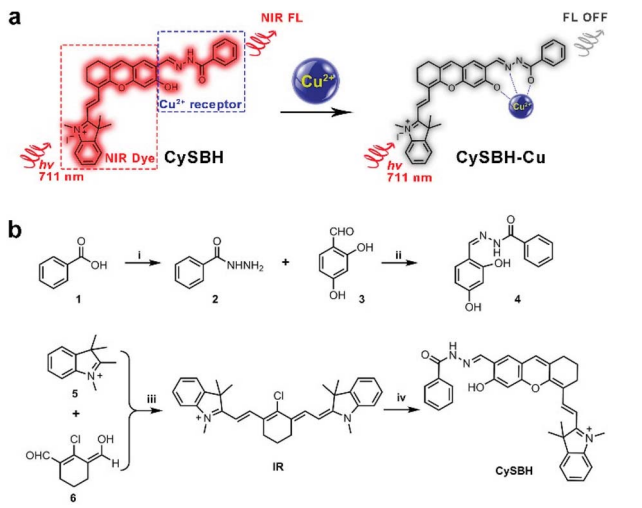

Scheme 1 (a) Chemical structure and proposed activation mechanism of the probe CySBH mediated by Cu^{2+}. (b) Synthesis of CySBH. Conditions: (i) thionyl chloride, EtOH, hydrazine hydrate; (ii) EtOH, r.t.; (iii) sodium acetate trihydrate, acetic anhydride, 75 °C; (iv) K_2CO_3, CH_3CN, 60 °C.

2. Experimental

2.1 Materials and instruments

Benzoic acid and 2,4-dihydroxybenzaldehyde were obtained from J&K Scientific Co., Ltd (Beijing, China). Copper chloride ($CuCl_2$), cuprous chloride (CuCl), zinc chloride ($ZnCl_2$), calcium chloride ($CaCl_2$) and mercury dichloride ($HgCl_2$) were purchased from Tianjin Kemiou Chemical Reagent Co., Ltd (Tianjin, China). Ferric chloride ($FeCl_3 \cdot 6H_2O$), manganese chloride ($MnCl_2$), nickel chloride hexahydrate ($NiCl_2 \cdot 6H_2O$), potassium chloride (KCl) and sodium chloride (NaCl) were purchased from Rionlon Bohua Pharmaceutical & Chemical Co., Ltd (Tianjin, China). All other chemicals were purchased from qualified reagent supplies with analytical reagent grade and used without further purification.

The NMR spectra were recorded on a Bruker AVANCE III-400 spectrometer, and the chemical shifts of ^1H NMR were expressed in parts per million downfield relative to the internal tetramethylsilane (δ = 0 ppm). High-resolution electrospray ionization mass spectra (HR-ESIMS) were acquired on a Bruker microTOF-Q II mass spectrometer (Bruker Daltonics, Billerica, MA). UV-vis extinction spectra were recorded on a UVvis spectrophotometer (PerkinElmer, Waltham, USA). The fluorescence spectra were measured on a fluorescence spectrophotometer (Fluoromax-4, HORIBA, USA). Fluorescence images of cells were acquired on an Olympus Fluoview 1000 confocal laser scanning microscope (Olympus, Tokyo, Japan). Whole-body *in vivo* fluorescence images and *ex vivo* fluorescence images of different organs of mice were obtained using a VISQUE™ *In Vivo* Elite Preclinical Optical Imaging System (Vieworks Co., Ltd Korea). Ultrapure water was prepared by an OKP purification system (Shanghai Laikie Instrument Co., Ltd, China).

2.2 Synthesis of compound 4

A mixture of 2,4-dihydroxybenzaldehyde (1.38 g) and benzhydrazide (1.36 g) in ethanol (50 mL) was stirred at room temperature for 3 h. A large amount of precipitate was precipitated. The precipitate was collected and further purified to provide compound **4**. ^1H NMR (400 MHz, DMSO-d_6): δ 11.89 (s, 1H), 11.46 (s, 1H), 9.94 (s, 1H), 8.48 (s, 1H), 7.88 (d, J = 7.6 Hz, 2H), 7.48–7.56 (m, 3H), 7.27 (d, J = 8.4 Hz, 1H), 6.33 (d, J = 8.4 Hz, 1H), 6.30 (s, 1H). ^{13}C NMR (101 MHz, DMSO-d_6): δ 163.0, 161.2, 160.0, 149.7, 133.5, 132.3, 131.9, 129.0, 128.0, 111.0, 108.2, 103.2. HRMS calcd for $C_{14}H_{12}N_2Na$: 279.0740 $[M + Na]^+$; found, 279.0752 $[M + Na]^+$.

2.3 Synthesis of compound IR

For the synthesis of compound IR, a mixture of compound **5** (260 mg), sodium acetate trihydrate (408 mg) and compound **6** (0.9 g) in acetic anhydride (10 mL) was heated at 75 °C for 4 h under a nitrogen atmosphere. The mixture was cooled with green precipitation, which was collected by filtration. The mixture was cooled with a large amount of green precipitate. The precipitate was collected and further purified by column chromatography to provide compound IR as a dark green solid. ^1H NMR (400 MHz, DMSO-d_6): δ 8.23 (d, J = 14.0 Hz, 2H), 7.63

© 2022 The Author(s). Published by the Royal Society of Chemistry

Open Access Article. Published on 24 January 2022. Downloaded on 2/11/2026 10:11:22 PM.
This article is licensed under a Creative Commons Attribution-NonCommercial 3.0 Unported Licence.

(d, $J = 7.6$ Hz, 2H), 7.40–7.44 (m, 4H), 7.26–7.28 (m, 2H), 6.30 (d, $J = 14.0$ Hz, 2H), 3.68 (s, 6H), 2.70–2.72 (m, 4H), 1.83–1.85 (m, 2H), 1.66 (s, 12H). ^{13}C NMR (101 MHz, DMSO-d_6): δ 172.6, 147.6, 142.8, 142.6, 140.9, 128.5, 126.0, 125.1, 122.3, 111.4, 101.8, 48.8, 31.5, 27.3, 25.8, 20.4.

2.4 Synthesis of the probe CySBH

K_2CO_3 (552 mg) was added to a solution of compound IR (610 mg) and compound **4** (281 mg) in dry CH_3CN (10 mL). The mixture was stirred at 60 °C for 8 h under a nitrogen atmosphere. The solvent was evaporated, and the crude product was purified by column chromatography using CH_2Cl_2/MeOH (20 : 1) to provide compound CySBH as a dark blue solid. ^{1}H NMR (400 MHz, CD_3OD-$CDCl_3$): δ 8.59 (s, 1H), 8.34 (d, $J =$ 13.6 Hz, 1H), 8.20 (s, 1H), 7.91 (d, $J = 7.2$ Hz, 1H), 7.60 (s, 1H), 7.49–7.54 (m, 4H), 7.30–7.36 (m, 2H), 7.14 (t, $J = 7.6$ Hz, 1H), 7.00 (d, $J = 8.0$ Hz, 1H), 6.56 (s, 1H), 5.79 (d, $J = 13.6$ Hz, 1H), 3.47 (s, 3H), 2.72–2.75 (m, 2H), 2.61–2.64 (m, 2H), 1.90–1.92 (m, 2H), 1.70 (s, 6H). ^{13}C NMR (400 MHz, CD_3OD-$CDCl_3$): δ 170.7, 66.0, 163.1, 159.2, 146.0, 143.5, 142.1, 140.5, 138.6, 133.3, 132.3, 128.8, 128.8, 127.9, 127.4, 124.3, 122.5, 120.4, 116.1, 114.7, 109.5, 104.5, 97.1, 30.8, 28.7, 28.6, 24.7, 21.3. HRMS calcd for $C_{34}H_{32}N_3O_3$: 530.2438 $[M]^+$; found, 530.2426 $[M]^+$.

2.5 Preparation of stock solutions

Stock solutions (10 mM) of the chlorate salts of Cu^+, Mg^{2+}, Ca^{2+}, Ba^{2+}, Pb^{2+}, K^+, Na^+, Ni^{2+}, Fe^{3+}, Hg^{2+}, Zn^{2+}, Al^{3+}, Mn^{2+}, Ag^+, Cr^{3+}, Cd^{2+}, Li^+ and Cu^{2+} ions were prepared in distilled water. The stock solutions were then diluted to appropriate concentrations with PBS (10 mM, pH 7.4) for further use.

2.6 General procedures for UV-vis and fluorescence spectra methods

For the UV-vis absorption and fluorescence spectra of CySBH measurements, a 10 μM CySBH working solution in phosphate saline buffer (PBS, 10 mM, pH 7.4, 1% DMSO) was used. Various analytes were added to the working solution, and the reactions were performed at room temperature for different times. Finally, UV-vis absorption was measured in CH_3CN/PBS buffer (v/v = 1 : 1, 5 mM, pH 7.4), while fluorescence spectra were acquired in CH_3CN/PBS buffer (v/v = 1 : 1, 5 mM, pH 7.4). For comparison, the solution that did not contain any interfering metal ions (blank) was measured under the same conditions at the same time.

2.7 Cell cultures and imaging

Human non-small-cell lung cancer (A549) cells and human cervical cancer (HeLa) cells were purchased from Morey Biosciences, Inc., and the cells were cultured according to the reported method. Both A549 and HeLa cells were grown in 10% fetal bovine serum (FBS) at 37 °C under a 5% CO_2 atmosphere. For fluorescence microscopy, the cells were seeded on glass-bottom culture dishes and cultured in culture medium for 24 h, after which CySBH (5 μM) was added to the dishes and incubated at 37 °C for 30 min. The medium was then removed, and the dishes were washed with PBS buffer three times to remove the remaining CySBH. The cells were then incubated in the absence or presence of Cu^{2+} (20 μM) in culture medium for another 10 min at 37 °C. After that, fluorescence images were obtained by confocal laser scanning microscopy NIR channels (excitation wavelength at 633 nm and emission wavelength from 650 nm to 750 nm).

2.8 Cell viability assay

The cytotoxicity of CySBH against A549 and HeLa cells was assessed utilizing a standard MTT method. Typically, cells were seeded into 96-well plates. After incubation at 37 °C for 24 h, the medium was replaced by CySBH aqueous solutions at different concentrations (0, 10, 20, 50 and 100 μM). After incubating cells at 37 °C for 24 h, the medium was replaced with freshly prepared MTT (1 mg mL^{-1} in PBS) and incubated for 4 h. After removing the MTT medium solution, 100 μL of dimethyl sulfoxide (DMSO) was added to the cells. The plate was shaken for 10 min, and the optical density (OD) was monitored. Each of the experiments was performed five times.

2.9 Fluorescence imaging of CySBH *in vivo*

Chinese Kunming mice (male, 20–25 g) were purchased from Gansu Provincial Maternity and Child-care Hospital and used for the *in vivo* fluorescence imaging of CySBH. All animal experiments were approved by the Experimental Animal Use and Care Committee, Gansu Provincial Maternity and Child-care Hospital and in accordance with the principles of laboratory animal operation regulation. For *in vivo* fluorescence imaging studies, mice were anesthetized by isoflurane. The anesthetized mice were injected with PBS buffer, CySBH (10 μM), CySBH (10 μM) with Cu^{2+} (5 μM), CySBH (10 μM) with Cu^{2+} (10 μM) and CySBH (10 μM) with Cu^{2+} (15 μM) for 0.1 mL under 5 mm of the skin at the right hindlimb, respectively. Finally, the fluorescence imaging signals were collected on a VISQUE™ *In Vivo* Elite Preclinical Optical Imaging System using a 630–680 nm excitation filter and a 690–740 nm emission filter.

3. Results and discussion

3.1 Design, synthesis and characterization of CySBH

Hemicyanine dye derivatives with NIR absorption and emission have attracted great attention due to their distinct advantages, such as hypotoxicity, high photostability and high fluorescence quantum yield. We noticed that reducing the electron-donating ability of the oxygen atom at hemicyanine dye can endow the NIR fluorophore with unique fluorescent turn-off properties.[47] Therefore, we anticipated that introduction of a benzoyl hydrazine in the hemicyanine dye could form a special salicylaldehyde benzoyl hydrazone group on the fluorophore.

The obtained compound could serve not only as an effective complexing agent for copper ions but also as a selective NIR probe to monitor Cu^{2+} in living systems. The synthesis procedure of probe CySBH is shown in Scheme 1b. Compounds **4** and IR were synthesized at first. The probe CySBH was prepared by reacting compound **4** with IR under basic conditions. The

Open Access Article. Published on 24 January 2022. Downloaded on 2/11/2026 10:11:22 PM.
This article is licensed under a Creative Commons Attribution-NonCommercial 3.0 Unported Licence.

chemical structure of CySBH was fully characterized and is shown in the Experimental Section and the ESI.†

3.2 Spectroscopic properties

With CySBH in hand, its spectral responses toward Cu^{2+} were measured in CH_3CN-PBS buffer (1 : 1) solution. As shown in Fig. 1a, probe CySBH initially exhibited two strong absorption peaks at 711 and 650 nm (red line). After being treated with Cu^{2+}, significant spectral changes were observed. The characteristic absorption peaks of CySBH at 711 and 650 nm decreased, accompanied by two new blue-shifted absorption peaks at 690 and 637 nm (Fig. 1a, black line), and the solution color also changed from blue to cyan. Moreover, CySBH initially displays a strong fluorescence emission at 744 nm, but the addition of Cu^{2+} shows a 130-fold decrease in fluorescence intensity (Fig. 1b). These results suggest that probe CySBH is highly sensitive to Cu^{2+}. The response time of the CySBH probe toward Cu^{2+} was studied by measuring the fluorescence intensity at 744 nm in real time. As shown in Fig. 1d, the fluorescence signal decreases instantaneously upon the addition of Cu^{2+} and reaches a plateau within 1.8 s. This result suggests that the coordination interaction between Cu^{2+} and CySBH can reach equilibrium very quickly. The sharp quenching of the original fluorescence signal of CySBH after incubation with Cu^{2+} could be ascribed to the fact that the salicylaldehyde benzoyl hydrazone group in CySBH can be efficiently coordinated with Cu^{2+}, which reduces the electron-donating ability of the oxygen atom. The photostability of organic probes is crucial for practical applications in bioimaging. Therefore, the photostability of the CySBH probe was investigated by time-sequential scanning. As shown in Fig. S1,† after 1800 s of continuous irradiation with a 711 nm laser, negligible obvious fluorescence intensity changes were observed. These results indicated that the probe CySBH had sufficient photostability and can be used as an excellent NIR imaging agent for bioimaging. After that, the fluorescence titration of CySBH toward Cu^{2+} was carried out to examine the possibility of quantitative analysis of Cu^{2+}. As shown in Fig. 1c, the addition of increasing amounts of Cu^{2+} triggered a gradual decrease in the fluorescence intensity at 744 nm when excited at a wavelength of 711 nm. The significant fluorescence on-off property suggests that the probe CySBH has excellent sensitivity toward Cu^{2+}. Furthermore, plotting the fluorescence intensity at 744 nm against the concentration of Cu^{2+} resulted in a logarithmic response curve (Fig. 1c, inset), and a good linear equation ($R^2 = 0.994$) was obtained in the Cu^{2+} concentration range from 0 to 2.5 μM, which can be used for the quantification of Cu^{2+} concentration. The detection limit ($3S/m$, in which S is the standard deviation of blank measurements, $n = 10$, and m is the slope of the linear equation) was calculated as 28.4 nM.

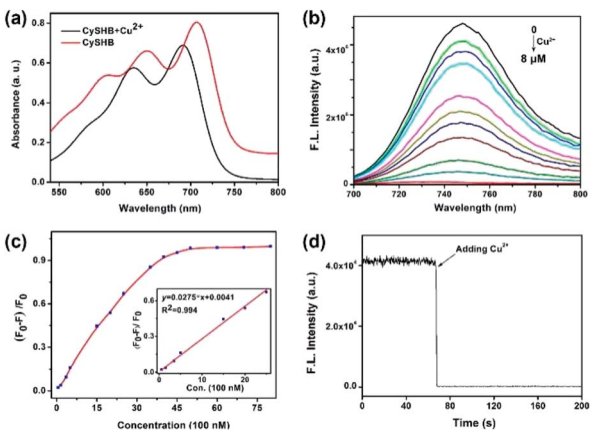

Fig. 1 (a) UV-vis absorption spectra of CySBH (5 μM) before (red line) and after addiction of Cu^{2+} (8 μM, black line) in acetonitrile/PBS (5 mM PBS, 1 : 1, v/v; pH = 7.4). (b) Fluorescence spectra of CySBH (5 μM) after adding different concentrations of Cu^{2+} (0–8 μM) in acetonitrile/PBS (5 mM PBS, 1 : 1, v/v; pH = 7.4), λ_{ex} = 690 nm. (c) Plot of the fluorescence emission intensity of CySBH (5 μM) at 744 nm toward the concentration of Cu^{2+}. Inset: calibration curve in the concentration range of 0–2.5 μM Cu^{2+}. F_0 and F are the fluorescence intensities of CySBH (5 μM) in acetonitrile/PBS (5 mM PBS, 1 : 1, v/v; pH = 7.4) in the absence and presence of Cu^{2+}, respectively. λ_{ex} = 690 nm. (d). Real-time fluorescence intensity of CySBH (5.0 μM) at 744 nm (λ_{ex} = 711 nm) upon the addition of Cu^{2+} (5 μM) in acetonitrile/PBS (5 mM PBS, 1 : 1, v/v; pH = 7.4).

3.3 Selectivity studies

The selectivity ability of the probe CySBH toward various potential interfering metal ions, including Cu^{+}, Mg^{2+}, Ca^{2+}, Ba^{2+}, Pb^{2+}, K^{+}, Na^{+}, Ni^{2+}, Fe^{3+}, Hg^{2+}, Zn^{2+}, Al^{3+}, Mn^{2+}, Ag^{+}, Cr^{3+}, Cd^{2+} and Li^{+}, was investigated. As shown in Fig. 2a, negligible fluorescence signal changes were observed when probe CySBH was added with the above substances under the same spectral conditions. In contrast, the fluorescence intensity ratio of CySBH increased nearly 130-fold after the addition of Cu^{2+}. These results suggest that CySBH is highly sensitive and specific to Cu^{2+} ions in the presence of other metal ions. Competitive experiments were further employed with various metal ions to confirm the practical evaluation of CySBH as a selectivity probe for Cu^{2+}. As shown in Fig. 2b, the addition of Cu^{2+} to the mixture of CySBH with different metal ions caused a significant increase in the fluorescence intensity ratio. These results show that the existence of excessive interference ions had little effect on the fluorescence response of CySBH to Cu^{2+}, confirming the high selectivity of CySBH for the Cu^{2+} ion.

3.4 Stoichiometric reaction of the probe with Cu^{2+}

It has been well documented that salicylidene acylhydrazone Schiff bases are one of most important π-conjugated ligands for Cu^{2+}.[38,44] In Schiff bases, the lone pair electrons of nitrogen and oxygen atoms in Schiff bases can occupy the 3d, 4s, and 4p empty electron orbitals of Cu^{2+} to form stable coordination complexes. In this work, we surmised that the nitrogen and oxygen atoms in Schiff bases could cooperate with Cu^{2+} to induce intramolecular electron transfer from the hemicyanine fluorophore moiety to Cu^{2+}, resulting in the NIR fluorescence signal being quenched. The interaction between CySBH and Cu^{2+} was investigated by mass spectrometry and Job's plot. As shown in Fig. 3a, the HRMS results of the CySBH and Cu^{2+} complex provide the characteristic pecks of 591.1562 belonging

© 2022 The Author(s). Published by the Royal Society of Chemistry

Open Access Article. Published on 24 January 2022. Downloaded on 2/11/2026 10:11:22 PM.
This article is licensed under a Creative Commons Attribution-NonCommercial 3.0 Unported Licence.

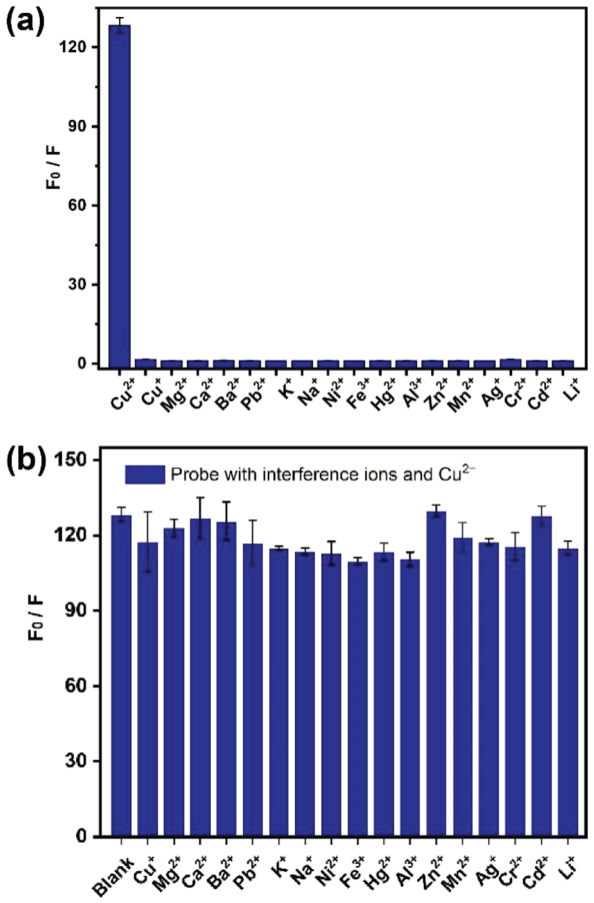

Fig. 2 (a) Selectivity of the probe CySBH (5 μM) toward Cu^{2+} over 17 different metal ions (20 μM). (b) Competitive tests of CySBH (5 μM) toward various potential interfering metal ions (50 μM Cu^{+}, Mg^{2+}, Ca^{2+}, Ba^{2+}, Pb^{2+}, K^{+}, Na^{+}, Ni^{2+}, Fe^{3+}, Hg^{2+}, Al^{3+}, Zn^{2+}, Mn^{2+}, Ag^{+}, Cr^{2+}, Cd^{2+} and Li^{+}) in acetonitrile/PBS (5 mM PBS, 1 : 1, v/v; pH = 7.4) with Cu^{2+} (10 μM). F_0 and F are the fluorescence intensities of CySBH (5 μM) in acetonitrile/PBS (5 mM PBS, 1 : 1, v/v; pH = 7.4) in the absence and presence of different concentrations of Cu^{2+}, respectively. λ_{ex} = 711 nm.

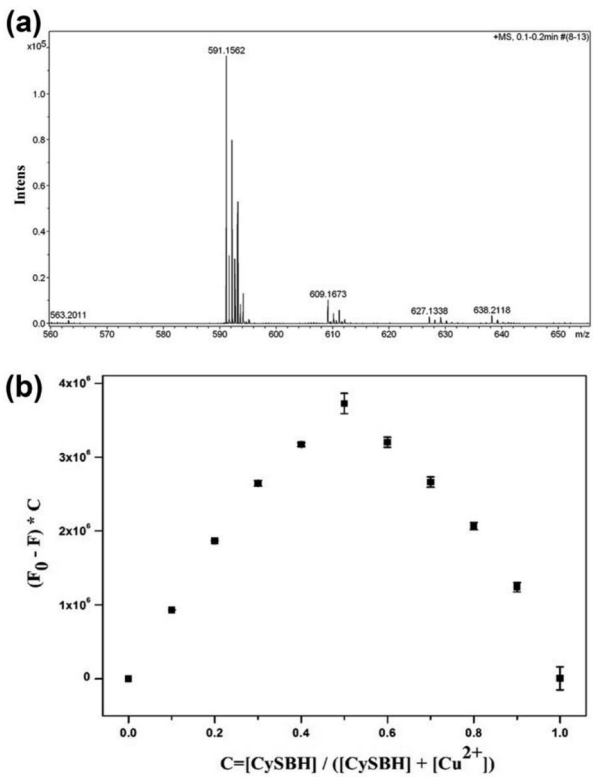

Fig. 3 (a) HRMS spectra of CySBH after the addition of Cu^{2+}. (b) Job's plot of the coordination ratio between CySBH and Cu^{2+}. The fluorescence intensity at 744 nm was plotted as a function of the molar ratio (Cu^{2+}/[CySBH + Cu^{2+}]) (the total concentrations of CySBH and Cu^{2+} were 10 μM).

to ([*m*/*z* CySBH] + [Cu^{2+}]-2H), which confirms the existence of the 1:1 complex. In addition, the continuous variation method (Job's plot) was carried out to further verify the stoichiometry between CySBH and Cu^{2+}. The differences in the fluorescence intensity before (F_0) and after (F) the addition of Cu^{2+} at 744 nm exhibited a maximum at ~0.5 (Fig. 3b), suggesting that the binding stoichiometry between CySBH and Cu^{2+} is 1:1. These results indicate the formation of a complex with 1:1 stoichiometric binding.

3.5 Effect of pH

Considering whether the probe can efficiently detect Cu^{2+} under varied pH values, the impact of pH on the sensing Cu^{2+} of CySBH was investigated. As shown in Fig. S2,† the fluorescence intensity of CySBH showed an obvious change over a wide pH range from 5 to 10 after the addition of Cu^{2+}. Furthermore, the probe CySBH exhibited a remarkable fluorescence change under a neutral environment (pH = 7.0), which is beneficial for further application in living systems.

3.6 Method comparison

The performance of CySBH is investigated in terms of excitation/emission wavelength, limit of detection, selectivity and response time. A detailed comparison between CySBH and some related Cu^{2+} probes reported in recent years is shown in Table S1.† Compared with the Cu^{2+} probes in the list, the NIR probe proposed in this study has excellent selectivity and short response times, which can be attributed to the Cu^{2+} selective recognition group based on salicylidene acylhydrazone Schiff bases. In addition, the NIR emission characteristics of CySBH make it more suitable for the imaging analysis of Cu^{2+} in living systems. Taken together, these results suggested that CySBH can be used as an effective and promising tool to monitor Cu^{2+} ions in living systems.

3.7 Fluorescence imaging in living cells

Since we have proven that the CySBH probe can detect Cu^{2+} specifically among various potential interfering metal ions in an isolated chemical environment, its application as a fluorescent probe for monitoring Cu^{2+} in living cells was further investigated. First, to evaluate the possibility of CySBH being applied

Open Access Article. Published on 24 January 2022. Downloaded on 2/11/2026 10:11:22 PM.
This article is licensed under a Creative Commons Attribution-NonCommercial 3.0 Unported Licence.

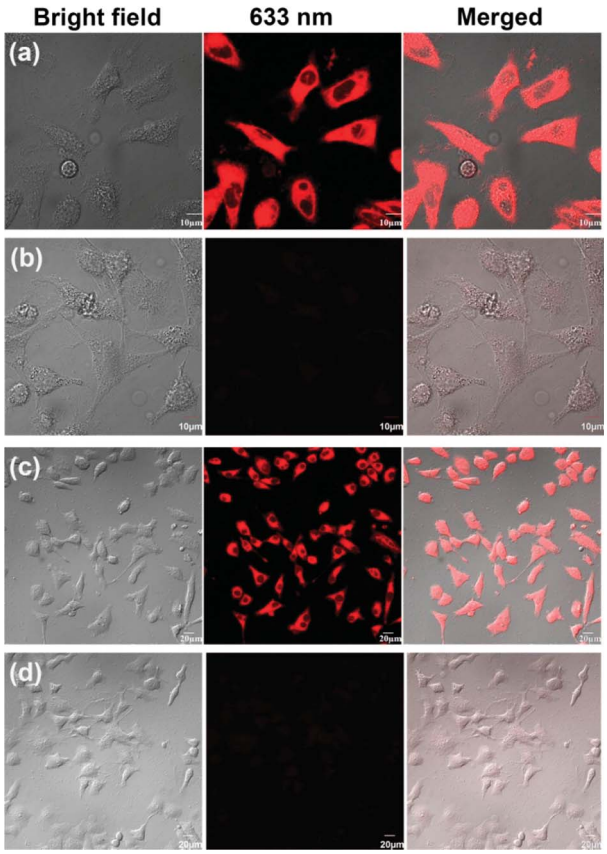

Fig. 4 Fluorescence images of probe CySBH in the A 549 and HeLa cells. (a) and (c) are the corresponding images of A549 and HeLa cells incubated with CySBH (5 μM) for 30 min, respectively. (b) Images of A549 cells incubated with CySBH (5 μM) for 30 min and then further treated with Cu^{2+} (20 μM) for 10 min. (d) Images of HeLa cells incubated with CySBH (5 μM) for 30 min and then further treated with Cu^{2+} (20 μM) for 10 min.

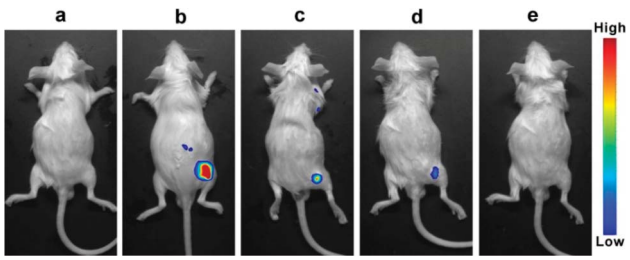

Fig. 5 *In vivo* fluorescence imaging of Cu^{2+} in KM mice. (a) Control; (b) mice given an injection of CySBH (10 μM); (c) mice given an injection of CySBH (10 μM) with Cu^{2+} (5 μM); (d) mice given an injection of CySBH (10 μM) with Cu^{2+} (10 μM); (e) mouse given an injection of CySBH (10 μM) with Cu^{2+} (15 μM). ($n = 3$).

to the living system, the *in vitro* cytotoxicity of CySBH was evaluated by a standard MTT assay with HeLa and A549 cells. As shown in Fig. S3,† when HeLa and A549 cells were incubated with different concentrations of CySBH ranging from 0 to 100 μM for 24 h, both cell lines showed high cell viability, indicating the low cytotoxicity and favorable biocompatibility of CySBH. After that, the capability of CySBH to image Cu^{2+} in HeLa and A549 cells was determined. As shown in Fig. 4a and c, significant intracellular fluorescence signals were observed in both HeLa and A549 cells after incubation with CySBH (5 μM) at 37 °C for 30 min, demonstrating that CySBH had good cell permeability. However, when further treated with Cu^{2+} in the culture medium for another 10 min and washed with PBS to remove extracellular Cu^{2+}, the intracellular fluorescence signals decreased dramatically in these cells (Fig. 4b and d). In fact, the A549 and HeLa cells after being treated with Cu^{2+} exhibited significantly lower fluorescence intensity than the untreated cells, with a P value less than 0.001 (Fig. S4†). This could be ascribed to the fact that the Cu^{2+} ion can effectively coordinate with CySBH in living cells and quench the fluorescence signal of CySBH. These results implied that CySBH can monitor Cu^{2+} sensitively and quickly in living cells.

3.8 *In vivo* fluorescence imaging of Cu^{2+} in mice

Near-infrared light can penetrate tissue deeply and has low background auto-fluorescence interference from biosystems. Since the probe CySBH displays favorable response properties toward Cu^{2+} *in vitro*, we simultaneously investigated the concentration-dependent response of CySBH toward Cu^{2+} in a living system *via* an *in vivo* fluorescence imaging method. Kunming mice were selected as the model and allocated into five groups. Fluorescence images *in vivo* were obtained using an *in vivo* optical imaging system. The first group of mice was treated with PBS buffer as a control group. As shown in Fig. 5a, there was no fluorescence emission when the mice were injected with PBS buffer. The second group of mice was treated with CySBH solution as a positive group. A strong fluorescence signal with a low background signal was observed in the right hindlimb of mice in the second group (Fig. 5b). The other groups of mice were treated with CySBH and Cu^{2+} at different concentrations. Interestingly, as the concentrations of Cu^{2+} injected with CySBH increased from 5 to 15 μM, the fluorescence intensity of the mice decreased gradually and was quenched after injection with 15 μM Cu^{2+} (Fig. 5c–e). This could be due to the effective complexation of Cu^{2+} ions and CySBH *in vivo*, which quenches fluorescence. These results suggest that the probe CySBH was practically effective and promising for monitoring and tracking Cu^{2+} ions *in vivo*.

4. Conclusions

In summary, we have developed a novel NIR probe for Cu^{2+} detection *in vitro* and *in vivo* by incorporating the benzoyl hydrazone unit into a hemicyanine dye. The coordination of the CySBH salicylaldehyde benzoyl hydrazone group with Cu^{2+} induces the deprotonation of the phenol group, resulting in the distinct quenching of the fluorescence intensity. By taking advantage of the specific coordination, CySBH exhibits high sensitivity and selectivity toward Cu^{2+}. The detection limit of CySBH for Cu^{2+} was as low as 28.4 nM. Moreover, since the probe CySBH has a long excitation wavelength (NIR) and favorable biocompatibility, the probe has been successfully

© 2022 The Author(s). Published by the Royal Society of Chemistry

Open Access Article. Published on 24 January 2022. Downloaded on 2/11/2026 10:11:22 PM.
This article is licensed under a Creative Commons Attribution-NonCommercial 3.0 Unported Licence.

applied in the bioimaging and detection of Cu^{2+} in diverse living cells and mice. We believe that this probe holds promising utility for bioimaging and diagnosing Cu^{2+}-associated diseases.

Conflicts of interest

There are no conflicts to declare.

Acknowledgements

This work was financially supported by the Health Industry Scientific Research Project of Gansu Province (No. GSWSKY2020-70), the scientific research start-up funds for openly recruited doctors of Gansu Agricultural University (No. GAU-KYQD-2019-23), National Natural Science Foundation of China (No. 21804135), and Natural Science Foundation of Gansu Province (20JR5RA133).

References

1 A. V. Davis and T. V. O'Halloran, A place for thioether chemistry in cellular copper ion recognition and trafficking, *Nat. Chem. Biol.*, 2008, **4**, 148–151.
2 T. Hirayama, G. C. Van de Bittner, W. G. Lawrence, S. Lutsenko and C. G. Chang, Near-infrared fluorescent sensor for *in vivo* copper imaging in a murine Wilson disease model, *Proc. Natl. Acad. Sci. U. S. A.*, 2012, **109**, 2228–2233.
3 J. Liu, Z. Liu, W. Wang and Y. Tian, Real-time tracking and sensing of Cu^{+} and Cu^{2+} with a single SERS probe in the live brain: toward understanding why copper ions were increased upon ischemia, *Angew. Chem., Int. Ed.*, 2021, **60**, 21351–21359.
4 E. Madsen and J. D. Gitlin, Copper and iron disorders of the brain, *Annu. Rev. Neurosci.*, 2007, **30**, 317–337.
5 Z. Aydin, B. Yan, Y. Wei and M. Guo, A novel near-infrared turn-on and ratiometric fluorescent probe capable of copper(II) ion determination in living cells, *Chem. Commun.*, 2020, **56**, 6043–6046.
6 T. Shu, Z. Yang, Z. Cen, X. Deng, Y. Deng, C. Dong and Y. Yu, A novel ratiometric fluorescent probe based on a BODIPY derivative for Cu^{2+} detection in aqueous solution, *Anal. Methods*, 2018, **10**, 5755–5762.
7 N. Solovyev, M. Vinceti, P. Grill, J. Mandrioli and B. Michalke, Redox speciation of iron, manganese, and copper in cerebrospinal fluid by strong cation exchange chromatography-sector field inductively coupled plasma mass spectrometry, *Anal. Chim. Acta*, 2017, **973**, 25–33.
8 J. Hu, R. E. Sturgeon, K. Nadeau, X. Hou, C. Zheng and L. Yang, Copper ion assisted photochemical vapor generation of chlorine for its sensitive determination by sector field inductively coupled plasma mass spectrometry, *Anal. Chem.*, 2018, **90**, 4112–4118.
9 A. Ramdass, V. Sathish, E. Babu, M. Velayudham, P. Thanasekaran and S. Rajagopai, Recent developments on optical and electrochemical sensing of copper(II) ion based on transition metal complexes, *Coord. Chem. Rev.*, 2017, **343**, 278–307.
10 H. Wang, Q. Lu, M. Li, H. Li, Y. Liu, H. Li, Y. Zhang and S. Yao, Electrochemically prepared oxygen and sulfur co-doped graphitic carbon nitride quantum dots for fluorescence determination of copper and silver ions and biothiols, *Anal. Chim. Acta*, 2018, **1027**, 121–129.
11 J. C. Jin, J. Wu, G. P. Yang and Y. Y. Wang, A microporous anionic metal-organic framework for a highly selective and sensitive electrochemical sensor of Cu^{2+} ions, *Chem. Commun.*, 2016, **52**, 8475–8478.
12 G. J. Park, G. R. You, Y. W. Choi and C. Kim, A naked-eye chemosensor for simultaneous detection of iron and copper ions and its copper complex for colorimetric/fluorescent sensing of cyanide, *Sens. Actuators, B*, 2016, **229**, 257–271.
13 B. Li, G. Lai, H. Zhang, S. Hu and A. Yu, Copper chromogenic reaction based colorimetric immunoassay for rapid and sensitive detection of a tumor biomarker, *Anal. Chim. Acta*, 2017, **963**, 106–111.
14 D. Udhayakumari, S. Naha and S. Velmathi, Colorimetric and fluorescent chemosensors for Cu^{2+}. A comprehensive review from the years 2013–15, *Anal. Methods*, 2017, **9**, 552–578.
15 Y. P. Dai, P. Wang, J. X. Fu, K. Yao, K. X. Xu and X. B. Pang, A quinoline-based Cu^{2+} ion complex fluorescence probe for selective detection of inorganic phosphate anion in aqueous solution and its application to living cells, *Spectrochim. Acta, Part A*, 2017, **183**, 30–36.
16 J. Li, D. Yim, W. D. Jang and J. Yoon, Recent progress in the design and applications of fluorescence probes containing crown ethers, *Chem. Soc. Rev.*, 2017, **46**, 2437–2458.
17 Y. S. Hu, J. Kang, P. P. Zhou, X. Han, J. Y. Sun, S. D. Liu, L. W. Zhang and J. G. Fang, A elective colorimetric and red-emitting fluorometric probe for sequential detection of Cu^{2+} and H_2S, *Sens. Actuators, B*, 2018, **255**, 3155–3162.
18 R. Kaushik, R. Sakla, N. Kumar, A. Ghosh, V. D. Ghule and D. A. Jose, Multianalytes sensing probe: fluorescent moisture detection, smartphone assisted colorimetric phosgene recognition and colorimetric discrimination of $Cu^{2+}$and Fe^{3+} ions, *Sens. Actuators, B*, 2021, **328**, 129026.
19 Y. Huang, C. F. Li, W. J. Shi, H. Y. Tan, Z. Z. He, L. Zheng, F. Liu and J. W. Yan, A near-infrared BODIPY-based fluorescent probe for ratiometric and discriminative detection of Hg^{2+} and Cu^{2+} ions in living cells, *Talanta*, 2019, **198**, 390–397.
20 Z. Li, Y. Xu, H. Xu, M. Cui, T. Liu, X. Ren, J. Sun, D. Deng, Y. Gu and P. Wang, A dicyanomethylene-4*H*-pyran-based fluorescence probe with high selectivity and sensitivity for detecting copper(II) and its bioimaging in living cells and tissue, *Spectrochim. Acta, Part A*, 2021, **244**, 118819.
21 Y. Li, Y. Zhao, W. Chan, Y. Wang, Q. You, C. Liu, J. Zheng, J. Li, S. Yang and R. Yang, Selective tracking of lysosomal Cu^{2+} ions using simultaneous target- and location-activated fluorescent nanoprobes, *Anal. Chem.*, 2015, **87**, 584–591.

© 2022 The Author(s). Published by the Royal Society of Chemistry

Open Access Article. Published on 24 January 2022. Downloaded on 2/11/2026 10:11:22 PM.
This article is licensed under a Creative Commons Attribution-NonCommercial 3.0 Unported Licence.

22 L. Yuan, W. Lin, S. Zhao, W. Gao, B. Chen, L. He and S. Zhu, A unique approach to development of near-infrared fluorescent sensors for *in vivo* imaging, *J. Am. Chem. Soc.*, 2012, **134**, 13510–13523.

23 X. Zhen, J. Zhang, J. Huang, C. Xie, Q. Miao and K. Pu, Macrotheranostic probe with disease-activated near-infrared fluorescence, photoacoustic, and photothermal signals for imaging-guided therapy, *Angew. Chem., Int. Ed.*, 2018, **57**, 7804–7808.

24 P. Llano-Suárez, D. Bouzas-Ramos, J. M. Costa-Fernández, A. Soldado and M. T. Fernández-Argüelles, Near-infrared fluorescent nanoprobes for highly sensitive cyanide quantification in natural waters, *Talanta*, 2019, **192**, 463–470.

25 Y. Tian, Y. Li, W. L. Jiang, D. Y. Zhou, J. Fei and C. Y. Li, In-situ imaging of azoreductase activity in the acute and chronic ulcerative colitis mice by a near-infrared fluorescent probe, *Anal. Chem.*, 2019, **91**, 10901–10907.

26 Y. Tian, Y. Li, W. X. Wang, W. L. Jiang, J. Fei and C. Y. Li, Novel strategy for validating the existence and mechanism of the "gut–liver axis" *in vivo* by a hypoxia-sensitive NIR fluorescent probe, *Anal. Chem.*, 2020, **92**(6), 4244–4250.

27 K. Huang, D. Han, X. Li, M. Peng, X. Zeng, L. Jiang and D. Qin, A new Cu^{2+}-selective fluorescent probe with six-membered spirocyclic hydrazide and its application in cell imaging, *Dyes Pigm.*, 2019, **171**, 107701.

28 Y. Liu, Q. Su, M. Chen, Y. Dong, Y. Shi, W. Feng, Z. Y. Wu and F. Li, Near-infrared upconversion chemodosimeter for *in vivo* detection of Cu^{2+} in Wilson disease, *Adv. Mater.*, 2016, **28**, 6625–6630.

29 F. Chen, F. Xiao, W. Zhang, C. Lin and Y. Wu, Highly Stable and NIR luminescent Ru-LPMSN hybrid materials for sensitive detection of Cu^{2+} *in vivo*, *ACS Appl. Mater. Interfaces*, 2018, **10**, 26964–26971.

30 X. Tang, J. Han, Y. Wang, L. Ni, L. Li, L. Wang and W. Zhang, A fluorescent chemosensor for Cu^{2+} ions and its application in cell imaging, *Tetrahedron*, 2017, **73**, 1367–1373.

31 B. Valeur and I. Leray, Design principles of fluorescent molecular sensors for cation recognition, *Coord. Chem. Rev.*, 2000, **205**, 3–40.

32 D. Wu, L. Chen, W. Lee, G. Ko, J. Yin and J. Yoon, Recent progress in the development of organic dye based near-infrared fluorescence probes for metal ions, *Coord. Chem. Rev.*, 2018, **354**, 74–97.

33 Y. Li, M. Sun, K. Zhang, Y. Zhang, Y. Yan, K. Lei, L. Wu, H. Yu and S. Wang, A near-infrared fluorescent probe for Cu^{2+} in living cells based on coordination effect, *Sens. Actuators, B*, 2017, **243**, 36–42.

34 H. Zhang, L. Feng, Y. Jiang, Y. T. Wang, Y. He, G. Zheng, J. He, Y. Tian, H. Sun and D. Ho, A reaction-based near-infrared fluorescent sensor for Cu^{2+} detection in aqueous buffer and its application in living cells and tissues imaging, *Biosens. Bioelectron.*, 2017, **94**, 24–29.

35 P. Li, X. Duan, Z. Z. Chen, Y. Liu, T. Xie, L. B. Fang, X. R. Li, M. Yin and B. Tang, A near-infrared fluorescent probe for detecting copper(II) with high selectivity and sensitivity and its biological imaging applications, *Chem. Commun.*, 2011, **47**, 7755–7757.

36 K. C. Ko, J. S. Wu, H. J. Kim, P. S. Kwon, J. W. Kim, R. A. Bartsch, J. Y. Lee and J. S. Kim, Rationally designed fluorescence 'turn-on' sensor for Cu^{2+}, *Chem. Commun.*, 2011, **11**, 3165–3167.

37 R. L. Sheng, P. F. Wang, Y. H. Gao, Y. Wu, W. M. Liu, J. J. Ma, H. P. Li and S. K. Wu, Colorimetric test kit for Cu^{2+} detection, *Org. Lett.*, 2008, **21**, 5015–5018.

38 Y. H. Zhao, Y. Lio, H. Wang, H. Wei, T. Cuo, H. Tian, L. Yuan and X. B. Zhang, A novel ratiometric and reversible fluorescence probe with a large Stokes shift for Cu^{2+} based on a new clamp-on unit, *Anal. Chim. Acta*, 2019, **1065**, 134–141.

39 Y. H. Zhao, Y. Li, Y. Long, Z. Zhou, Z. Tang, K. Deng and S. Zhang, Highly selective fluorescence turn-on determination of fluoride ions *via* chromogenic aggregation of a silyloxy-functionalized salicylaldehyde azine, *Tetrahedron Lett.*, 2017, **58**, 1351–1355.

40 B. Tharmalingam, M. Mathivanan, G. Dhamodiran, K. S. Mani, M. Paranjothy and M. Murugesapandian, Star-shaped ESIPT-active mechanoresponsive luminescent AIEgen and its on-off-on emissive response to Cu^{2+}/S^{2-}, *ACS Omega*, 2019, **4**, 12459–12469.

41 Y. Xu, L. Yang, H. Wang, Y. Zhang, X. Yang, M. Pei and G. Zhang, A new "off-on-off" sensor for sequential detection of Al^{3+} and Cu^{2+} with excellent sensitivity and selectivity based on different sensing mechanisms, *J. Photochem. Photobiol., A*, 2020, **391**, 112372.

42 W. Nasomphan, P. Tangboriboonrat and S. Smanmoo, Dansyl based "Turn-On" fluorescent sensor for Cu^{2+} ion detection and the application to living cell imaging, *J. Fluoresc.*, 2017, **27**, 2201–2212.

43 X. Pan, J. Jiang, J. Li, W. Wu and J. Zhang, Theoretical design of near-infrared Al^{3+} fluorescent probes based on salicylaldehyde acylhydrazone Schiff base derivatives, *Inorg. Chem.*, 2019, **58**, 12618–12627.

44 W. Shan, F. Liu, J. Liu, Y. Chen, Z. Yang and D. Guo, Synthesis and luminescence properties of salicylaldehyde isonicotinoyl hydrazone derivatives and their europium complexes, *J. Inorg. Biochem.*, 2015, **150**, 100–107.

45 S. Kumar and M. Nath, New diorganotin(IV) complexes of salicylaldehyde based hydrazones bearing furan heterocycle moiety: X-ray structural investigation of dimethyltin(IV) and diphenyltin(IV) complexes, *J. Organomet. Chem.*, 2018, **856**, 87–99.

46 S. Sharma and K. S. Ghosh, Recent advances (2017–20) in the detection of copper ion by using fluorescence sensors working through transfer of photo-induced electron (PET), excited-state intramolecular proton (ESIPT) and Förster resonance energy (FRET), *Spectrochim. Acta, Part A*, 2021, **254**, 119610.

47 H. Chen, P. Yang, Y. Li, L. Zhang, F. Ding, X. He and J. Shen, Insight into triphenylamine and coumarin serving as copper(II) sensors with "OFF" strategy and for bio-imaging in living cells, *Spectrochim. Acta, Part A*, 2020, **224**, 117384.

© 2022 The Author(s). Published by the Royal Society of Chemistry